論文 8-4-28

자연대류 영향을 고려한 상변화 열에너지 저장장치의 열전도향상에 관한 수치적 연구

Numerical Study on Enhanced Heat Conduction of Phase-Change Thermal Energy Storage Devices in The Presence of Natural Convection

정 홍 철*
Hong-Chul Chung

ABSTRACT

Numerical inverstigation of heat transfer in phase-change energy storage devices was performed in order to aid in the design process for a finned Phase-Change Material(PCM). A simplified model based on a quasi-linear, transient, thin fin equation, which predicts the fraction of melted phase-change material, and the shape of liquid-solid interface as a function of time, is used. The model is solved by using Finite Volume Method(FVM), and the numerical results have showed good agreement with experimental data.

국문요약

상변화 에너지 저장장치는 변동하는 액체-고체 상접합면과 자연대류의 존재에 기인한 비선형성 때문에 해석적으로 분석하기가 어렵다. 핀(fin) 형태의 상변화 에너지 저장장치를 준선형화 시켜 열전달을 수치적으로 해석하여 실험 데이타와 비교 검증하였다. 대칭형 수평 핀에 대하여 준선형, 비정상의 얇은 2 차원적 모델을 세우고 유한체적방법(FVM)에 의해 시간의 함수로 융해된 상변화물질의 비율과 액체-고체 상접합면의 형상을 예측하였다. 유한체적방법(FVM)에 의한 결과는 실험결과와 비교적 잘 일치하였다. 벽과 융해점 사이의 온도차가 클수록 융해된 상변화물질의 비율은 증가하였으며 대류항을 포함하는 경우가 없는 경우보다 실험결과에 더 가까운 해를 얻을 수 있었다.

* Department of Aeronautical Engineering Hankuk Aviation University

Nomenclature

c_p	specific heat
h	heat transfer coefficient
H	latent heat of fusion
k	thermal conductivity
L	length
q	heat flux
t	time
T	temperature
V	volume
β	thermal expansion coefficient
μ	dynamic viscosity
ρ	density

Subscripts

c	cell
cond.	conduction
f	x direction fin length
i	arbitrary node
l	property of the liquid phase
lim	convergence limit
m	property of the metal fin
m. p.	phase-change material melting point
s	property of the solid phase
sens	sensible
w	denotes value at the wall($x = 0$)

1. Introduction

Phase-change energy storage devices have an inherent disadvantage due to the insulating properties of the PCM used. Such systems are difficult to analyze theoretically due to the nonlinearities of the moving liquid-solid interface and the presence of natural convection. In this study the difficulty is removed using the simplified quasi-linear, transient, thin fin equation and the equation determining the rate of interface recession. Figure 1 shows an example of how fins might be incorporated in a PCM storage device. The purpose of this study is to develop and test a simplified model for the prediction of the melting rate and the melting interface location in a finned phase-change energy storage device. This is achieved by analyzing the elemental symmetry cell, shown in Fig. 2, found in such a system. The proposed model is sloved by FVM[1], and once the predictions are validated comparing with experimental data[2),4)], the model could be used as a low cost design tool to predict the relative effects of fin length, fin thickness, spacing between fins, and physical properties of both PCM and fin material on the dynamic benavior of a finned PCM storage device.

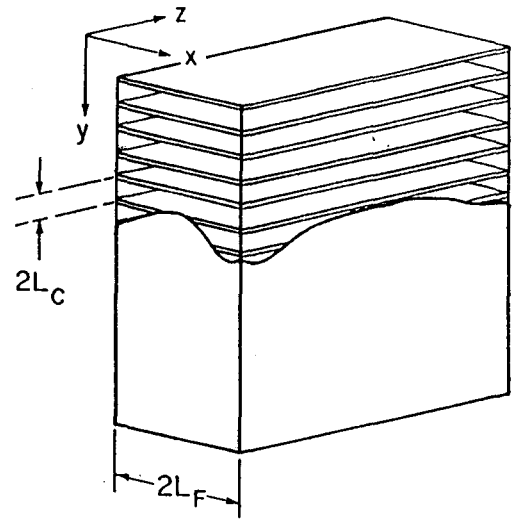

Fig. 1 An Example of a Phase-Change Energy Storage Device Incorporating Horizontal Metal Fins

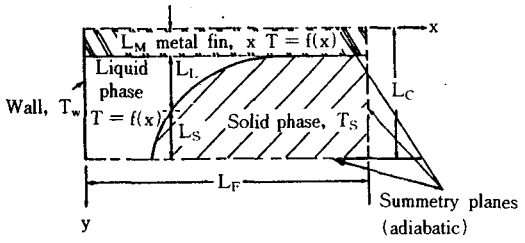

Fig. 2 Elemental Symmetry Cell for a Horizontally Finned Phase-Change Energy Storage Device

2. Governing Equations

An energy balance conducted on an arbitrary differential element dx, shown in Fig. 3b, yields two equations which are the basis for the model.

The energy balance of the metal fin as the first equation becomes

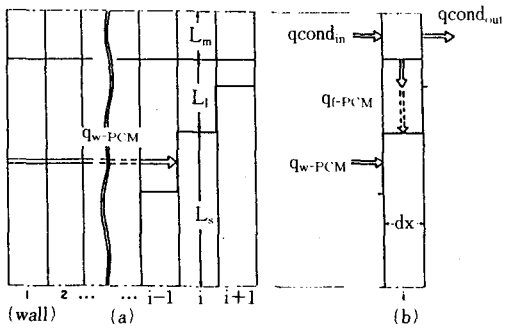

Fig. 3 a) A Representation of the Discretized System in which L_l is Allowed a Continuous Value at Each Node
b) Energy Fluxes on an Arbitrary Slice of the Symmetry Cell

$q_{f-sens} = q_{cond(net)} + q_{f-PCM}$

Rewrite more specifically as

$$(\rho C_p)_m L_m \frac{\partial T}{\partial t} = k_m L_m \frac{\partial^2 T}{\partial x^2} - h(TT_{m.p.}) \cdots\cdots (1)$$

where Tis the fin temperature which a function of fin length and time.

Melting of the PCM proceeds due to energy transferred from two distinct sources, the fin and the constant temperature end wall. The rate of interface recession can be found the following equation :

$$H\rho_s \frac{\partial L_l}{\partial t} dx = h(TT_{m.p.})\, dx + \frac{k_l}{x}(T_w T_{m.p.}) \frac{\partial L_l}{\partial x} dx \cdots\cdots (2)$$

Nondimensional form of Eqs. (1) and (2) can be written as follows.

$$\frac{\partial \theta}{\partial \tau} = \frac{\partial^2 \theta}{\partial \eta^2} - \frac{\lambda^2 k \mathrm{Nu}_c}{\psi} \theta \cdots\cdots (3)$$

$$\frac{\partial \gamma}{\partial \tau} = \xi k \left(\lambda^2 \mathrm{Nu}_c \theta + \frac{1}{\eta} \frac{\partial \gamma}{\partial \eta} \right) \cdots\cdots (4)$$

where the dimensionless parameters are

$$Nu_c = \frac{hL_c}{k_l}, \quad \eta = \frac{x}{L_f}, \quad \lambda = \frac{L_f}{L_c}, \quad \gamma = \frac{L_l}{L_c},$$

$$\psi = \frac{k_l}{k_m}, \quad \theta = \frac{T - T_{m.p.}}{T_w - T_{m.p.}}$$

$$\tau = \frac{k_m t}{(\rho C_p)_m L^2_f},$$

$$\xi = \frac{(\rho C_p)_m T_w - T_{m.p.})}{H\rho_s}$$

3. Finite Volume Formulation

Introduce Taylor series expansion of θ about τ as following :

$$\theta^{n+1} = \theta^n + \Delta\tau \frac{\partial \theta^{n+1}}{\partial \tau} + O(\Delta\tau^2) \quad (5)$$

Substituting Eq. (3) in to(5) yields

$$\theta^{n+1} = \theta^n + \Delta\tau \left(\frac{\partial^2 \theta^{n+1}}{\partial \eta^2} - \frac{\lambda^2 k \mathrm{Nu}_c}{\psi} \theta^{n+1} \right) \cdots\cdots (6)$$

To take Finite Volume equation, the spatial integral of Eq. (6) becomes

$$\int \theta^{n+1} d\eta = \int \theta^n d\eta + \int \Delta\tau \left(\frac{\partial^2 \theta^{n+1}}{\partial \eta^2} - \frac{\lambda^2 k \mathrm{Nu}_c}{\psi} \theta^{n+1} \right) d\eta \cdots\cdots (7)$$

Integration by parts of the spatially derivative term of Eq. (7) gives

$$\int \Delta\tau \frac{\partial^2 \theta^{n+1}}{\partial \eta^2} d\eta = \Delta\tau \frac{\partial^2 \theta^{n+1}}{\partial \eta^2} \Big| \quad (8)$$

Using the summation notation Eq(7) can be written as

$$\Sigma \theta_i^{n+1} \Delta\eta = \Sigma \theta_i^n \Delta\eta + \Delta\tau \frac{\partial \theta_i^{n+1}}{\partial \eta} \Big|_{i-\frac{1}{2}}^{i+\frac{1}{2}}$$

$$- \Sigma \Delta \tau \frac{\lambda^2 k(\mathrm{Nu_c})_i}{\psi} \theta^{n+1}_i \Delta \eta \quad \cdots\cdots (9)$$

Rewriting Eq. (9) for a cell yields

$$\theta^{n+1}_i = \theta^n_i + \frac{\Delta \tau}{\Delta \eta} \left(\frac{\theta^{1+1}_{i+1} - \theta^{1+1}_i}{\Delta \eta} - \frac{\theta^{1+1}_i - \theta^{1+1}_{i-1}}{\Delta \eta} \right) - \Delta \tau \frac{\lambda^2 k(\mathrm{Nu_c})_i}{\psi} \theta^{n+1}_i \quad \cdots\cdots (10)$$

or

$$\Delta \tau \, \theta^{n+1}_{i+1} + \left(-2\Delta \tau - \Delta \eta^2 - \Delta \tau \, \Delta \eta^2 \frac{\lambda^2 k(\mathrm{Nu_c})_i}{\psi}\right) \theta^{n+1}_i + \Delta \tau \, \theta^{n+1}_{i-1} = -\Delta \eta^2 \theta^n_i \quad \cdots\cdots (11)$$

Similarly, the Finite Volume Formulation of Eq. (4), which determines the rate of interface recession, becomes as following :

$$\int \gamma^{n+1} d\eta = \int_{\eta} \gamma^n d\eta + \int \Delta \tau \, \xi k \lambda^2 \mathrm{Nu_c} \theta^{n+1} d\eta + \frac{\Delta \tau \, \xi k}{\eta} \gamma^n \Big| \quad \cdots\cdots (12)$$

For a cell Eq. (12) gives

$$\gamma^{n+1}_i = \gamma^n_i + \Delta \tau \, \xi k \lambda^2 (\mathrm{Nu_c})_i \theta^{n+1}_i + \frac{\Delta \tau \, \xi k}{\eta \, \Delta \eta} (\gamma^n_{i+1} - \gamma^n_i) \quad \cdots\cdots (13)$$

Calculation procedure

1) Find the Rayleigh number which is related to the Nusselt number.

$$Ra_c = \frac{g \beta (T_w - T_{m.p.}) \rho^2_l (C_p)_l L^3_c}{\mu k_l}$$

The local Rayleigh number Ra is determined from the following equation

$Ra_i = (Ra_c \theta \gamma^3)_i$

In natural convection, the heat transfer coefficient is related to Rayleigh number as follows :

$Nu_i = 1$ for $Ra_i \leq$ Rayleigh stability limit

$Nu_i = ARa^n$ for $Ra_i >$ Rayleigh stability limit

where A and are coefficients determined by experiments conducted for a particular geometry. The normal Rayleigh stability limit for horizontal paralled plates without any wall effects is about 1700. This was the value used throughout the numerical study. In the present system, it is not the side walls which are reducing natural convection, but the influence of the flow in neighboring differential element may be reduced by a reverse flow or stagnant region near by. For this reason, a standard correlation for horizontal parallel plates will over-predict the heat transfer coefficient for the pressent geometry. The coefficient A = 0.4753 and the ecponent n = 0.1 are determined by a trial and error procedure to agree with experimental data[4] for one run.

Nu is converted $\mathrm{Nu_c}$ by the following relation.

$$\mathrm{Nu_c} = \frac{\mathrm{Nu}}{\gamma + L_{cond}}$$

where L_{cond} is a conduction length parameter used to avoid singularties associated with startup conditions. A value of $L_{cond} = 0.22$ was used throughout the numerical study. This value was determined by a trial and error procedure which compared the model predicition to experimental data[4] for the initial conduction regime in one experimental run.

2) Solve the implicit Finite Volume Eq. (11) for finding temperature distribution along the fin with inelt boundary condition $\theta = 1$ at $\eta = 0$.
3) With the temperature distribution of the fin determine the rate of liquid-solid interface recession in Eq. (13).
4) Iterate the above procedure until γ has converged to within a predeterminted convergence limit, γ_{lim}, everywhere in the system.
5) Once γ has converged, Eq. (11) is solved again, and the procedure advances to the next time level(n+1).

Care must be taken to avoid overmelting of the PCM. If overmelting has occurred, then γ is forced to its maximum value at that node. The

numerical predictions presented were run using $\Delta\eta = 0.05$, $\Delta\tau = 0.1$, and $\gamma_{lim} = 0.01$. Physical properties of n-octadecane as the PCM and aluminum as the fin are used.

4. Results and Discussion

Fig. 4 presents a convergence history of FVM for melt fraction with the natural log of Root Mean Square(RMS) errors in various ΔT. As ΔT increases, the number of iteration of reach the steady state decreases.

The temperature variation along the fin in various ΔT is shown in Fig. 5 The fin temperature decreases with increasing the x and ΔT.

The liquid-solid interface profile(γ) can be determined using a spatially one dimensional(η) set of nodes for a different ι. Thus, this model can predict the percent of model PCM(melt fraction) as a function of ι. In other words, melt fraction can be calculated from the plotting of interface profile versus nodes at each time.

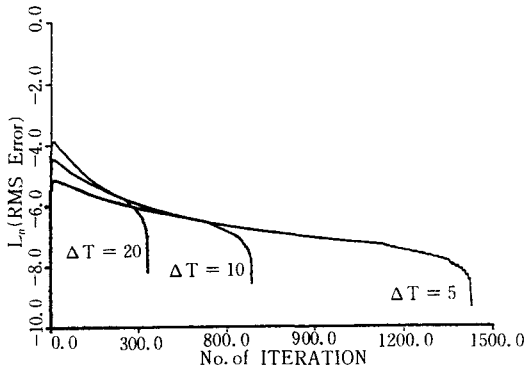

Fig. 4 Convergence history of FVM for melt fraction in variout ΔT

Fig. 6 compares the numerical results shown by solid lines to the experimental data poltted symbols for $L_m = 1/8$ ″ with various ΔT. The model is successful at quantitatively predicting the effects of different ξ caused by different ΔT.

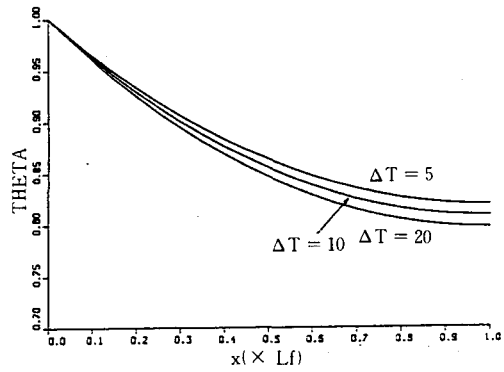

Fig. 5 Temperature variation along the fin for various ΔT

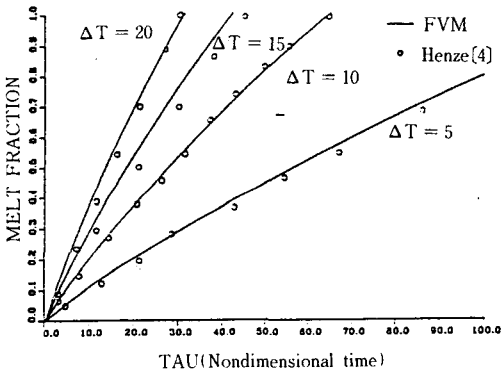

Fig. 6 Comparison of model predictions and experimental data for melt fraction vs. time for L_m = 1/8″ and various ΔT

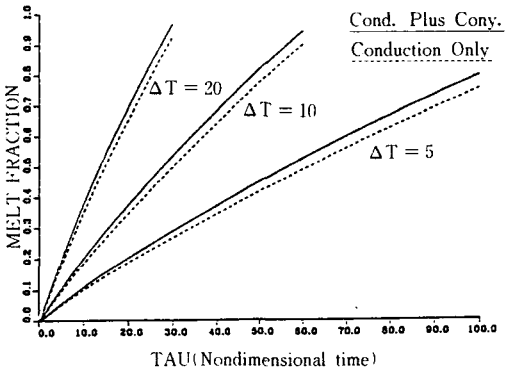

Fig. 7 Model predictions of conduction only and conduction plus natural convection for various ΔT

For the horizontally finned geometry considered in this study, the magnitude of heat transfer due to natural convection depends on L_c, L_m, and ΔT, the parameters which influence Ra. An example of the magnitude of these effects on the melting rate for $L_m = 1/8''$, and $\Delta T = 5$, 10, and 20℃, as predicted by the model is shown in Fig. 7. For each of the three cases, the upper curve is the natural convection result, which agrees with the experimental data as shown in Fig. 6. The lower curves are the model predictions for pure conduction only, for the same 3 runs.

5. Conclusion

Applying finite volume method(FVM) to the heat transfer in phase-change energy storage devices, the following conclusion was obtained :

1) Simplified model for the solid/liquid phase change problem and its solution by the FVM showed quite a good agreement with the experimental data.
2) As the temperature differences between wall and melting point, the melt fraction is larger.
3) More accurate prediction could be obtained by including convection term in addition to conduction term.

REFERENCES

1) M. G. Hall; Cell Vertex Multigrid Schemes for Solution of the Euler Equations; Numerical Methods for Fluid Dynamics Ⅱ; Oxford University Press, pp. 303~345; 1986.
2) W. R. Humphries; Performance of Finned Thermal Capacitors; NASA T. N. D-7690; July 1974.
3) W. R. Humphries and E. I. Griggs; A Design Handbook for Phase Change Thermal Control and Energy Storage Devices; NASA T. P. 1074; Nov. 1977.
4) R. H. Henze; Enhanced Heat Conduction in Phase-Change Thermal Energy Storage Devices; Master's Thesis;
5) E. M. Sparrow, S. V. Patankar, and S. Ramdhyani; Analysis of Melting in the Presence of Natural Convection in the Melt Region; Journal of Heat Transfer, v. 99, pp. 520~526; Nov. 1977.